Lattice vibrations and structural instability in caesium near the cubic-to-tetragonal transition

2000 J. Phys.: Condens. Matter 12 8973

(http://iopscience.iop.org/0953-8984/12/42/304)

J. Phys.: Condens. Matter **12** (2000) 8973–8982. Printed in the UK PII: S0953-8984(00)16451-3

Lattice vibrations and structural instability in caesium near the cubic-to-tetragonal transition

Y Kong and O Jepsen

Max-Planck-Institut für Festkörperforschung, Heisenbergstrasse 1, D-70569 Stuttgart, Germany

Received 17 August 2000, in final form 18 September 2000

Abstract. Under pressure, caesium undergoes a transition from a high-pressure fcc (face-centred cubic) phase (Cs-II) to a collapsed fcc phase (Cs-III) near 4.2 GPa. At 4.4 GPa there follows a transition to the tetragonal Cs-IV phase. In order to investigate the lattice vibrations in the fcc phase and seek a possible dynamical instability of the lattice, the phonon spectra of fcc Cs at volumes near the III-to-IV transition are calculated using Savrasov's density functional linear-response LMTO (linear muffin-tin orbital) method. Compared with quasiharmonic model calculations including non-central interatomic forces up to second neighbours, at the volume $V/V_0 = 0.44$ (V_0 is the experimental volume of bcc Cs (bcc $\equiv$ body-centred cubic) with $a_0 = 6.048$ Å), the linear-response calculations show soft intermediate-wavelength $T_{[1\bar{1}0]}[\xi\xi 0]$ phonons. Similar softening is also observed for short-wavelength L[$\xi\xi\xi$] and L[00ξ] phonons and intermediate-wavelength L[$\xi\xi\xi$] phonons. The Born–von Kármán analysis of the dispersion curves indicates that the interplanar force constants exhibit oscillating behaviours against plane spacing n and the large softening of intermediate-wavelength $T_{[1\bar{1}0]}[\xi\xi 0]$ phonons results from a negative (110) interplanar force constant $\Phi_{n=2}$. The calculated frequencies for high-symmetry K and W and longitudinal X and L phonons decrease with volume compression. In particular, the frequencies of the $T_{[1\bar{1}0]}[\xi\xi 0]$ phonons with ξ around $1/3$ become imaginary and the fcc structure becomes dynamically unstable for volumes below $0.41V_0$. It is suggested that superstructures corresponding to the $\boldsymbol{q} \neq 0$ soft mode should be present as a precursor of tetragonal Cs-IV structure.

1. Introduction

At ambient pressure caesium metal crystallizes in a bcc structure with experimental lattice parameter $a_0 = 6.048$ Å [1] at 0 K, obtained from the high-temperature values by extrapolation. It is a simple s^1 metal with nearly free-electron character. Under pressure the s valence electrons are transferred to more localized d-like states [2], and caesium exhibits an interesting sequence of phase transitions [3–8]. At the pressure 2.3 GPa a transition [3, 4] from bcc (Cs-I) to fcc (Cs-II) occurs with a small reduction of volume. Near 4.2 GPa, the fcc Cs-II phase undergoes an isostructural transition [4] to a collapsed fcc phase Cs-III with a large volume reduction (9%). Then at 4.4 GPa there follows a transition to the tetragonal Cs-IV phase [5] with a decrease of the coordination number from 12 for Cs-III to 8 for Cs-IV (strictly, four nearest neighbours at 3.349 Å and four second-nearest neighbours at 3.542 Å at 8 GPa). At higher pressures more complicated phases [6–8] appear.

Many detailed investigations have been devoted to the study of the phase transitions in caesium, both experimentally (see reference [7] and literature cited therein) and theoretically (see, e.g., references [7–14]). The pressure-induced electronic s $\rightarrow$ d transition was believed to be the driving force for destabilizing the highly symmetric low-pressure structures (bcc or fcc) with respect to lower symmetry structures. The transition III $\rightarrow$ IV was attributed to the

0953-8984/00/428973+10$30.00

accelerated progress [5] of the s → d transition and the unusual decrease of the coordination number from Cs-III to Cs-IV has been interpreted in terms of directional bonding induced by the s → d transition [12, 15].

In general, the s → d electronic transition in caesium affects not only the static lattice properties by changing the electronic band structure but also the lattice vibrational properties by modifying the effective interatomic interactions. The structural behaviour of caesium may therefore be reflected in the phonon spectrum and it is therefore of interest to investigate the phononic behaviour with applied pressure. Glötzel and McMahan [11] suggested that an anomaly in the lattice vibrational contribution to the pressure is a possible mechanism for the isostructural II → III transition. Recently, Christensen *et al* [16] calculated phonon dispersions of fcc Cs within the quasiharmonic approximation to study the thermal expansion coefficient of caesium and the isostructural transition. They found that below $V/V_0 = 0.375$ (V_0 is the experimental volume of bcc Cs at ambient conditions) fcc Cs becomes unstable due to softening of a transverse [110] phonon branch, which is characterized by a negative shear elastic constant C'. Very recently, Xie *et al* [17] investigated the phonon instabilities of caesium using density functional perturbation theory. Their calculations showed that the instability of the fcc caesium occurs at a volume of about $0.46V_0$, which is also driven by a negative C'. However, it is not clear what happened with the phonons before the C' went soft. Using the density functional linear-response LMTO method [18], we calculate the accurate phonon spectrum of fcc Cs at the volumes near the III–IV transition to study the lattice vibrations in fcc Cs and to seek a possible dynamical instability of fcc Cs before C' becomes negative. According to our calculations, fcc Cs becomes unstable at a volume slightly smaller than $V/V_0 = 0.41$. Soft $T_{[1\bar{1}0]}[\xi\xi 0]$ phonons with $\xi \sim \frac{1}{3}$ are found to be responsible for the dynamical instability.

This paper is organized as follows. Some computational details concerning linear-response LMTO calculations are described in the next section. Section 3 presents the results obtained and some discussions. Firstly, the phonon dispersion curves for fcc Cs at the volume $V/V_0 = 0.44$ are analysed in terms of force constants between atoms; then the phonon frequencies at various volumes are discussed in relation to the instability of the fcc structure. Several concluding remarks are made in the last section.

2. Computational details

The density functional linear-response LMTO method [18] is used in the present study to calculate the phonon spectrum of fcc Cs at the volumes around the Cs-III–Cs-IV transition. Phonon dispersion curves for a large number of simple and transition metals and a few compounds have been calculated by the linear-response LMTO method, and excellent agreement with experimental data was obtained [18, 19]. In the following we summarize some details of the calculations.

The dynamical matrix of fcc Cs is calculated for a set of irreducible $\boldsymbol{q}$-points in a (8, 8, 8) reciprocal-lattice grid (29 points per 1/48th part of the Brillouin zone (BZ)). The (I, J, K) reciprocal-lattice grid is defined in the usual manner: $\boldsymbol{q}_{ijk} = (i/I)\boldsymbol{G}_1 + (j/J)\boldsymbol{G}_2 + (k/K)\boldsymbol{G}_3$, where $\boldsymbol{G}_i$ are the primitive translations in reciprocal space. We chose the exchange–correlation potential of Vosko–Wilk–Nusair [20] plus the non-local generalized-gradient-approximation (GGA-96) correction [21], because this gave a better prediction of the equilibrium volume at ambient pressure and 0 K which is only 4% smaller than the experimental zero-pressure volume at 0 K. On the other hand, the local density approximation (LDA) gave a nearly 20% overbinding at ambient pressure. The calculated bcc-to-fcc transition pressure of 2.0 GPa is in good agreement with the experimental value of 2.3 GPa [4].

In the calculations a 3κ–spd LMTO basis set is used with the one-centre expansions inside the non-overlapping muffin-tin (MT) spheres performed up to $l_{max} = 6$. In the interstitial region, the s, p and d basis functions are expanded in plane waves. The 5s semicore state is treated as valence state in a separate energy window. The induced charge densities and screened potentials are represented inside the MT spheres by spherical harmonics up to $l_{max} = 6$ and by plane waves with a 148.4 Ryd energy cut-off (9984 plane waves) in the interstitial region.

The $\boldsymbol{k}$-space integration is performed over a (16, 16, 16) grid (145 irreducible points) by means of the improved tetrahedron method [22], but the integration weights for these $\boldsymbol{k}$-points are calculated from a denser (32, 32, 32) grid (897 points in the irreducible BZ). This results in a more accurate representation of the Fermi surface with a small number of $\boldsymbol{k}$-points.

The phonons along the high-symmetry lines presented in the next section were calculated in a denser $\boldsymbol{q}$-mesh which fit to the (16, 16, 16) $\boldsymbol{k}$-grid.

3. Results and discussion

3.1. Phonon dispersions at $V/V_0 = 0.44$

Figure 1 shows the calculated phonon dispersion curves along some high-symmetry directions for fcc Cs at the volume $0.44V_0$, which is in the experimental volume range of the cubic-to-tetragonal phase transition. To the right the calculated phonon density of states (DOS) is plotted. The dashed lines represent the fitted results from the Born–von Kármán model which is described in the next section. The calculated phonon frequencies at the high-symmetry zone-boundary (ZB) points L, X, K and W are listed in table 1.

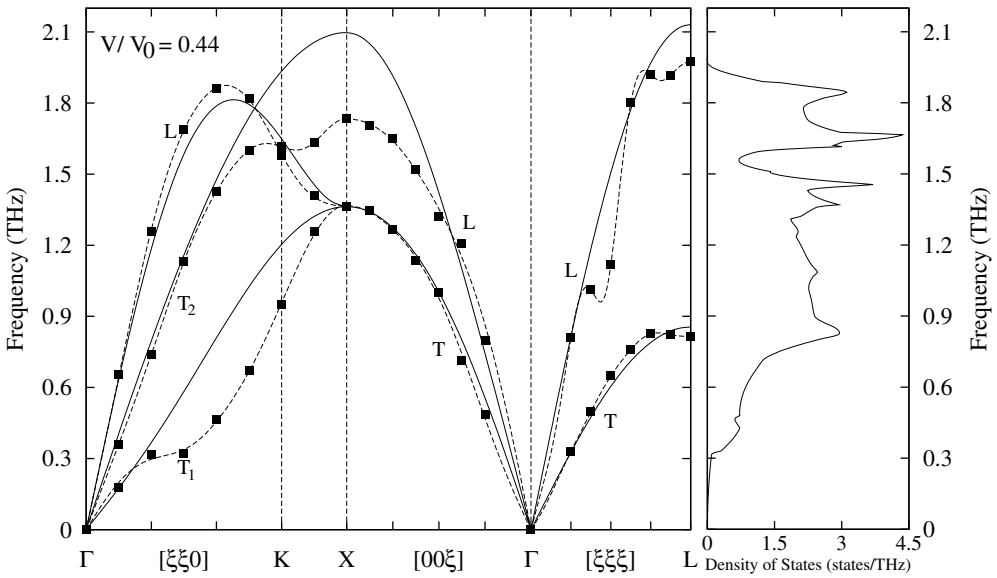

Figure 1. Calculated phonon dispersion curves along three symmetry directions for fcc Cs at the volume $V/V_0 = 0.44$. The squares show the results calculated using the density functional linear-response method and the solid lines represent the results from a quasiharmonic calculation (see the text). The dashed lines are the fitted results from the Born–von Kármán model. Also plotted, in the right-hand panel, is the phonon density of states derived from the linear-response calculations.

Table 1. Calculated phonon frequencies ν_i (THz) at the high-symmetry L, X, K and W points for fcc Cs at the volume $V/V_0 = 0.44$ and corresponding mode-Grüneisen parameters γ_i defined by $\gamma_i = -(\partial \ln \nu_i / \partial \ln V)$. Also listed in brackets are the frequencies from the short-range force model calculation.

		L	X	K	W
L branch	ν_i	1.97 (2.13)	1.73 (2.10)	1.58 (1.65)	1.51
	γ_i	−0.95	−0.79	−0.80	−1.27
T_1 branch	ν_i	0.82 (0.86)	1.36 (1.36)	0.95 (1.20)	1.23
	γ_i	0.71	0.49	−0.80	−1.60
T_2 branch	ν_i	0.82 (0.86)	1.36 (1.36)	1.62 (1.93)	1.46
	γ_i	0.71	0.49	−0.93	−1.41

As observed in figure 1, the phonon frequencies of the L[$\xi\xi$0], T[00ξ] and T[$\xi\xi\xi$] branches exhibit rather normal dispersion while the T[$\xi\xi$0], L[00ξ] and L[$\xi\xi\xi$] dispersion curves show abnormal behaviour for intermediate and short wavelengths, which indicates long-range interactions between atoms. For the L[$\xi\xi\xi$] phonon branch, a small downwards anomaly is seen around $\xi = \frac{1}{4}$. Near the zone boundary, the L[$\xi\xi\xi$] phonons have very little dispersion and the frequencies of the L[00ξ] phonons are rather small compared to those for other fcc metals. The T[$\xi\xi$0] phonons have flat regions around $\xi = \frac{1}{3}$ and $\frac{3}{4}$ for the polarizations [1$\bar{1}$0] (T_1) and [001] (T_2), respectively. Since the phonon DOS in figure 1 was calculated with a coarse (8, 8, 8) grid, these abnormal behaviours are not clearly seen in the DOS plotted. Nevertheless, the sudden increase of the DOS at a frequency just above 0.3 THz and the small sharp peak at a frequency near 1.6 THz indicate the presence of these anomalies.

In metals at equilibrium the long-range interatomic interactions are generally of little importance due to the screening effect of the electrons. The lattice dynamical properties of metals can therefore be described well using a short-range force model. This, however, may not hold for caesium under high pressure. The pressure-induced electronic s $\rightarrow$ d transition causes the valence charge density of caesium to deviate from spherical symmetry with a consequent reduction in the electronic screening and increased interactions between the atoms. To check this, we calculate the phonon dispersion curves of fcc Cs at the volume $V/V_0 = 0.44$ using a short-range force model within the quasiharmonic approximation. The dispersion relations are derived as in the usual harmonic approximation by considering non-central forces between atoms up to second neighbours and the four interatomic force constants involved in the dynamical matrices are obtained from the three calculated elastic constants† and the T[100] zone-boundary phonon frequency by expanding the elements of the dynamical matrix and finding its long-wavelength limit. The dispersion curves obtained are plotted in figure 1 as solid lines and the phonon frequencies at the zone boundaries are listed in table 1. Note that the quasiharmonic results presented here are derived from a short-range force model, which does not exactly consider the electronic contribution to the dynamical matrix. The difference from the results from linear-response calculations may therefore reveal the effects of long-range interatomic interactions. It may be seen in figure 1 that the short-range non-central force model describes the T[00ξ], T[$\xi\xi\xi$] and L[$\xi\xi$0] phonon dispersions quite well. However, the previously mentioned anomalies in the L[00ξ], L[$\xi\xi\xi$] and T[$\xi\xi$0] dispersion curves calculated by the linear-response method are not reproduced and they may therefore be a consequence of long-range interactions.

† The bulk modulus and shear moduli (C', C_{44}) of fcc Cs are calculated in a full-potential LMTO scheme. For the volume $0.44V_0$, $C_{11} = 13.8$ GPa, $C_{12} = 11.0$ GPa and $C_{44} = 8.1$ GPa.

In general, an abnormal behaviour of the phonon dispersion may be attributed to special properties of interatomic force constants. In the following subsection, we shall analyse the dispersion curves by using the Born–von Kármán model to find these special properties of the interactions between the atoms in fcc Cs.

3.2. Born–von Kármán analysis of force constants

Since one of the motivations of the present work is to interpret the anomalies in the calculated phonon dispersion curves for fcc Cs, it is necessary to use a model which can reproduce these anomalies. This could be achieved by a force-constant model based on the Born–von Kármán theory [23].

In the Born–von Kármán theory the frequencies $\nu(\boldsymbol{q})$ of the normal vibration modes for an fcc lattice with one atom per unit cell are given as the solutions of a 3×3 determinantal equation:

$$|4\pi^2 M\nu^2(\boldsymbol{q})\delta_{\alpha\beta} - C_{\alpha\beta}(\boldsymbol{q})| = 0 \tag{1}$$

where M is the mass of the atom and

$$C_{\alpha\beta}(\boldsymbol{q}) = \sum_{l'} \Phi_{\alpha\beta}(l,l')\exp[\mathrm{i}\boldsymbol{q}\cdot\boldsymbol{R}(l,l')] \tag{2}$$

where $\Phi_{\alpha\beta}(l,l')$ is the $\alpha\beta$-component of the force constant matrix for the atoms in the lth and l'th cells. For the phonon modes along the three high-symmetry directions $[\xi\xi0]$, $[00\xi]$ and $[\xi\xi\xi]$, the $C_{\alpha\beta}$-matrices are diagonal and the solution of equation (1) leads to equations in ν^2 of the form

$$4\pi^2 M\nu^2 = \sum_n \Phi_n[1-\cos(n\pi q/q_{max})] \tag{3}$$

where q_{max} is half the distance to the nearest reciprocal-lattice point in the direction of $\boldsymbol{q}$, $q = |\boldsymbol{q}|$ and Φ_n is a sum of $\Phi_{\alpha\beta}(l,l')$ [24] for which the phase $\boldsymbol{q}\cdot\boldsymbol{R}(l,l')$ is a constant. Φ_n effectively represents a force between a plane of atoms and the planes of atoms normal to $\boldsymbol{q}$ and n planes away. The summation includes N terms, so $\Phi_n = 0$ for $n > N$. Thus, a Fourier series analysis of the squares of the phonon frequencies will yield the interplanar force constants.

Accordingly, a least-squares Fourier fit is performed using equation (3) for the phonon dispersion curves of fcc Cs at the volume $0.44V_0$ obtained from linear-response calculations. The fitted dispersion curves are plotted in figure 1 as dashed lines. Within the accuracy of the calculated phonon frequencies, it is found that a satisfactory fit can only be obtained by including at least four planes in the $[00\xi]$ branches, five planes in the T$[\xi\xi\xi]$ branch and even six planes in the $[\xi\xi0]$ and L$[\xi\xi\xi]$ branches. In table 2 we list the fitted interplanar force

Table 2. Interplanar force constants Φ_n (up to $n = 6$) for fcc Cs at the volume $V/V_0 = 0.44$ in units of 10^{-3} Ryd Bohr^{-2}. The errors given are approximate errors for the fitted Φ_n. Note that a satisfactory fit for the $[00\xi]$ and T$[\xi\xi\xi]$ phonons is obtained only with four and five Fourier components, respectively.

	Φ_1	Φ_2	Φ_3	Φ_4	Φ_5	Φ_6	Error
T$[00\xi]$	10.69	0.11	−0.24	−0.18	—	—	± 0.15
L$[00\xi]$	16.09	1.85	0.72	0.29	—	—	± 0.50
T$[\xi\xi\xi]$	4.11	0.49	−0.36	0.10	−0.05	—	± 0.02
L$[\xi\xi\xi]$	23.09	−0.86	−2.44	3.35	1.39	−2.78	± 0.50
$T_{[001]}[\xi\xi0]$	16.32	3.56	−0.40	−1.06	0.80	−0.55	± 0.19
$T_{[1\bar{1}0]}[\xi\xi0]$	8.51	−4.10	1.74	−0.42	0.21	0.09	± 0.11
L$[\xi\xi0]$	8.88	14.52	1.29	−0.85	0.30	−0.29	± 0.12

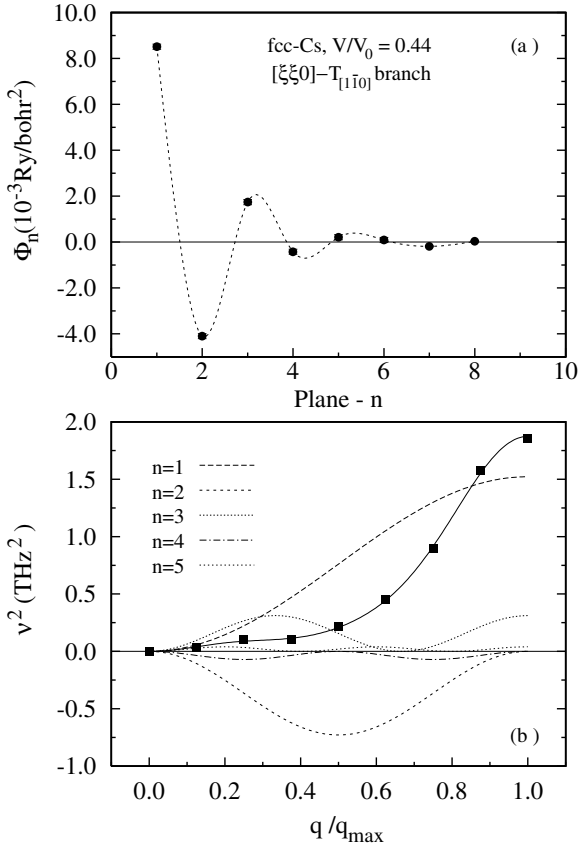

Figure 2. (a) The interplanar force constants (up to $n = 8$) for the $T_{[1\bar{1}0]}[\xi\xi 0]$ branch phonons of fcc Cs at the volume $V/V_0 = 0.44$. A clear oscillating behaviour against the plane number (interplanar spacing) is seen. (b) Values of ν^2 for the same branch phonons plotted as functions of the reduced wave-vector. The fitted curve (solid line) with eight planes is shown together with the contributions from the first five Fourier components.

constants Φ_n. Since four planes along the $[00\xi]$ direction correspond to interactions out to at least eighth-neighbour atoms and five (six) planes along the $[\xi\xi\xi]$ ($[\xi\xi 0]$) direction out to further neighbours, the fitted results confirm the presence of long-range interactions between atoms in fcc Cs. We plot the fitted Φ_n for the $T_{[1\bar{1}0]}[\xi\xi 0]$ branch in figure 2(a) as a function of n, which is effectively the distance between planes of atoms. The Φ_n are observed to oscillate with the distance between planes, especially with a prominently negative $\Phi_{n=2}$. The values of ν^2 for the same phonon branch and the fitted curve with $N = 8$ are shown in figure 2(b) together with the individual contributions from the first five Fourier components. It is seen that the $n = 2$ planes produce a largely negative contribution to the frequencies of phonons, which partly cancels the dominant contribution from the $n = 1$ planes. Consequently, the soft intermediate-wavelength $T_{[1\bar{1}0]}[\xi\xi 0]$ phonons result and a flat region of the dispersion curve is formed. A similar oscillating behaviour of the fitted Φ_n is seen in some of the other branches although this is less pronounced. The anomalies observed in the $T_{[001]}[\xi\xi 0]$ and $L[\xi\xi\xi]$ dispersion curves can be associated with these oscillations. For the $L[00\xi]$ branch no oscillations in Φ_n are found. The very low phonon frequencies for long wavelengths compared to the short-range model calculation may be attributed to the small value of $\Phi_{n=1}$.

The interplanar force constants can be used to derive interatomic force constants [24]. With a general force model, a linear least-squares fitting analysis for the Φ_n in table 2 only allows us to work out the interatomic force constants in fcc Cs extending to the fourth neighbour. The truncation of the interactions with further neighbours introduces large errors in the fitting procedure and makes the fitted interatomic force constants less reliable. Nevertheless, in table 3 we list the best-fit values of the interatomic constants for fcc caesium.

Table 3. The best-fit values of interatomic force constants for fcc Cs at the volume $V/V_0 = 0.44$ in units of Ryd Bohr^{-2}. The force constant notation follows the definition of Brockhouse *et al* [24].

Neighbour location	Force constants			Values (Ryd Bohr^{-2})
First	α_1	γ_1	0	$\alpha_1 = 21.2 \times 10^{-4}$
$(a/2)(1, 1, 0)$	γ_1	α_1	0	$\beta_1 = -2.0 \times 10^{-4}$
	0	0	β_1	$\gamma_1 = 38.6 \times 10^{-4}$
Second	α_2	0	0	$\alpha_2 = -2.1 \times 10^{-4}$
$(a/2)(2, 0, 0)$	0	β_2	0	$\beta_2 = 5.8 \times 10^{-4}$
	0	0	β_2	
Third	α_3	δ_3	γ_3	$\alpha_3 = 3.6 \times 10^{-4}$
$(a/2)(2, 1, 1)$	δ_3	β_3	γ_3	$\beta_3 = -0.6 \times 10^{-4}$
	γ_3	γ_3	β_3	$\gamma_3 = 3.6 \times 10^{-4}$
				$\delta_3 = -0.4 \times 10^{-4}$
Fourth	α_4	γ_4	0	$\alpha_4 = -0.4 \times 10^{-4}$
$(a/2)(2, 2, 0)$	γ_4	α_4	0	$\beta_4 = 0.04 \times 10^{-4}$
	0	0	β_4	$\gamma_4 = -4.1 \times 10^{-4}$

3.3. Soft modes and lattice instability

The volume dependences of the high-symmetry zone-boundary L, X, K and W phonons for fcc Cs are presented in figure 3. From this the mode-Grüneisen parameter $\gamma_i = -(\partial \ln \nu_i / \partial \ln V)$ was derived and the values are listed in table 1. It may be seen that all the high-symmetry phonons except the transverse X and L phonons decrease in frequency with increasing pressure and consequently have negative mode-Grüneisen parameters, which may be an indication that the fcc structure is unstable under pressure.

In figure 4 we show the $T_{[1\bar{1}0]}[\xi\xi 0]$ phonon dispersion curves of fcc Cs for the volumes $V/V_0 = 0.37, 0.40, 0.41$ and 0.44. At volumes between $V/V_0 = 0.41$ and 0.40 the phonon frequencies around $\xi = \frac{1}{3}$ become imaginary. However, the shear elastic constant C' does not become negative before the volume is reduced to $V/V_0 = 0.37$ where the entire phonon branch becomes unstable. Christensen *et al* [16] and Xie *et al* [17] inferred from their calculations that it is the pressure-induced negativity of C' which is the cause of the instability of the fcc phase. They however did not trace the development of the instability in detail and it is clear from figure 4 that it is a $\boldsymbol{q} \neq 0$ $T_{[1\bar{1}0]}[\xi\xi 0]$ soft mode which drives the dynamical instability of the fcc phase close to $V/V_0 = 0.41$. As a consequence of the soft mode, superstructures should exist as a precursor to the tetragonal Cs-IV phase transition. It is interesting to note that the calculated transition volume $V/V_0 = 0.41$–0.40 is close to the volume where the fcc-to-tetragonal transition is observed [5].

In figure 5 we illustrate the displacement pattern of atoms in fcc Cs corresponding a $T_{[1\bar{1}0]}[\frac{1}{4}\frac{1}{4}0]$ phonon mode and the resulting Cs superstructure. As seen from figure 5, a structural element of the displacement pattern is triangular prisms, which are also present

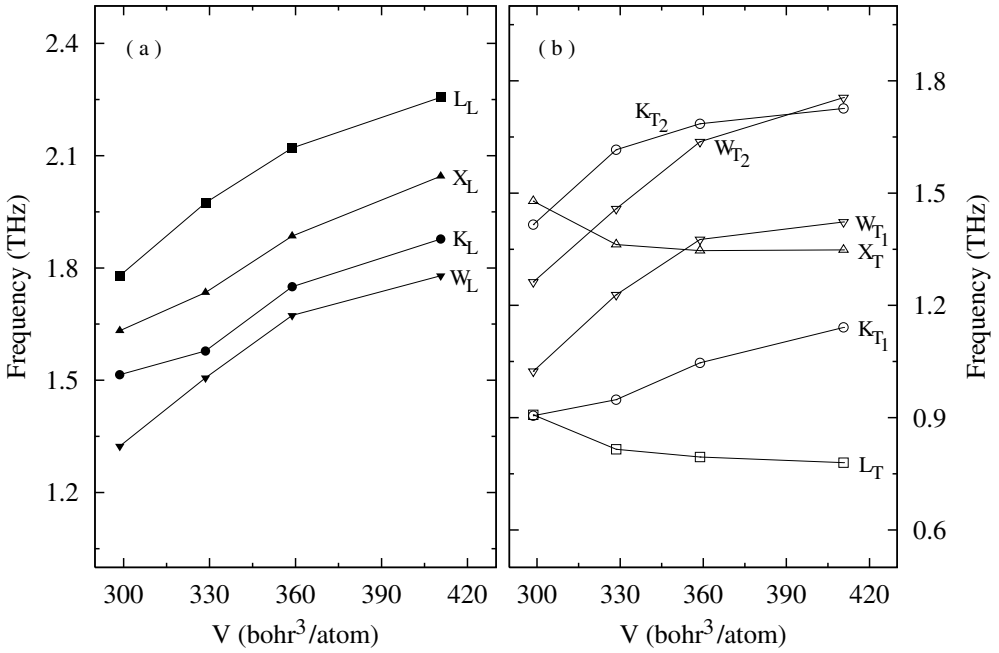

Figure 3. Calculated phonon frequencies ν_i (THz) at the high-symmetry L, X, K and W points for fcc Cs as a function of the volume. (a) Longitudinal and (b) transverse branches.

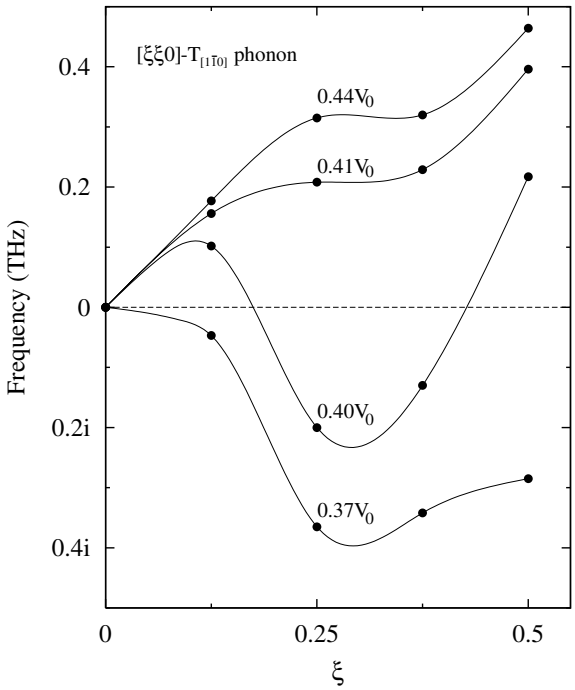

Figure 4. Calculated $T_{[1\bar{1}0]}[\xi\xi 0]$ phonon dispersion curves for fcc Cs at the volumes $V/V_0 =$ 0.37, 0.40, 0.41 and 0.44. The points are the calculated values and the lines result from the interpolation between points and are only a guide to the eye.

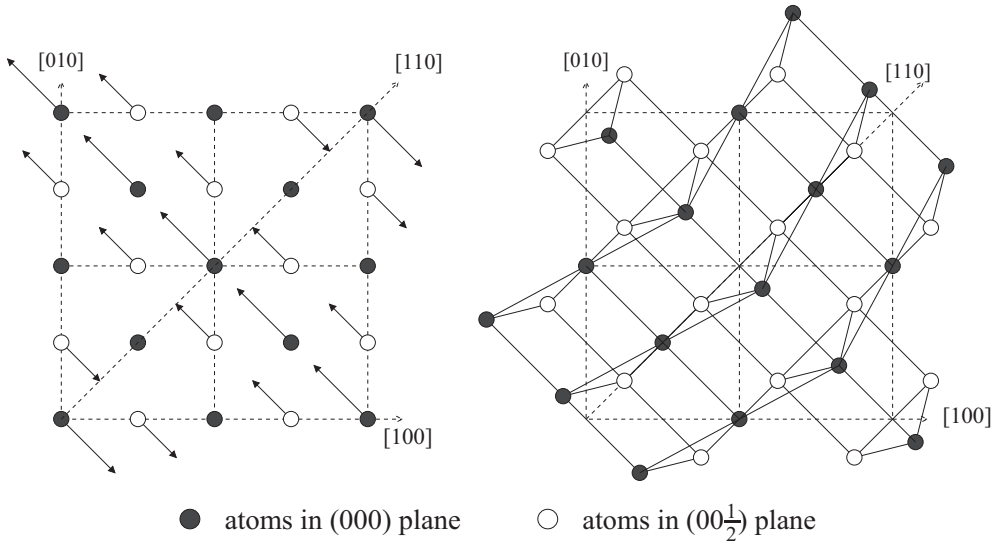

Figure 5. Schematic illustrations of the displacement pattern (left) of atoms in fcc Cs corresponding to a $T_{[1\bar{1}0]}[\frac{1}{4}\frac{1}{4}0]$ phonon and the resulting Cs superstructure (right). The lengths of the solid arrows are proportional to the displacements of the atoms and the dashed arrows indicate the [100], [010] and [110] directions of the fcc lattice.

in the Cs-IV structure, even though other possible soft modes as well as the coupling between phonons could be important.

Usually a soft phonon mode leads to a second-order or nearly first-order phase transition. Early experimental results [5] indicated that the Cs-III–Cs-IV transition is first order in character with a 4.3% volume reduction. Therefore soft phonon modes should not be considered the unique driving force in the caesium III–IV phase transformation even though the soft mode leads to an instability in the fcc structure. The changes of the electronic properties under pressure, such as the s–d transition, must play an important role.

4. Conclusions

Using a density functional linear-response LMTO method, we have studied the phonon spectra of fcc caesium at volumes near the III–IV transition. Several anomalies in the dispersion curves have been found.

Within the Born–von Kármán theory of lattice dynamics, the observed anomalies in the calculated phonon dispersion curves for fcc Cs at the volume $0.44V_0$ are connected with oscillating behaviours of the interplanar force constants against plane spacing n. In particular, a negative (110) interplanar force constant $\Phi_{n=2}$ is found to be responsible for the soft intermediate-wavelength $T_{[1\bar{1}0]}[\xi\xi 0]$ phonons.

The frequencies of high-symmetry K and W and longitudinal X and L phonons decrease with volume compression and the consequent negative mode-Grüneisen parameters indicate an instability of the fcc lattice under pressure. When the volume is below $0.41V_0$, the frequencies of the $T_{[1\bar{1}0]}[\xi\xi 0]$ phonons with ξ around $\frac{1}{3}$ become imaginary prior to the sign change of the shear elastic constant C' and the fcc lattice is thus dynamically unstable. It is suggested that superstructures corresponding to the $\boldsymbol{q} \neq 0$ $T_{[1\bar{1}0]}[\xi\xi 0]$ soft phonon should be present as a precursor of tetragonal Cs-IV structure. It was pointed out in reference [7] that the fcc structure

of Cs-III could not be confirmed and that Cs-III appears to be a rather complicated structure. The present argument may stimulate further experimental study based on re-examining the structure of Cs at the pressures near the Cs-II–Cs-III–Cs-IV transitions.

Acknowledgments

Y Kong gratefully acknowledges helpful discussions with and advice from Professor O K Andersen, and we are grateful to Professor K Syassen for a critical reading of the manuscript.

References

[1] Anderson M S, Gutman E J, Packard J R and Swenson C A 1969 *J. Phys. Chem. Solids* **30** 1587
[2] Sternheimer R M 1950 *Phys. Rev.* **78** 235
[3] Kennedy G C, Jayaraman A and Newton R C 1962 *Phys. Rev.* **126** 1363
[4] Hall H T, Merrill L and Barnett J D 1964 *Science* **146** 1297
[5] Takemura K, Minomura S and Shimomura O 1982 *Phys. Rev. Lett.* **49** 1772
[6] Takemura K, Shimomura O and Fujihisa H 1991 *Phys. Rev. Lett.* **66** 2014
[7] Schwarz U, Takamura K, Hanfland M and Syassen K 1998 *Phys. Rev. Lett.* **81** 2711
[8] Takemura K, Christensen N E, Novikov D L, Syassen K, Schwarz U and Hanfland M 1998 *Phys. Rev.* B **61** 14 399
[9] Louie S G and Cohen M L 1974 *Phys. Rev.* B **10** 3237
[10] McMahan A K 1978 *Phys. Rev.* B **17** 1521
[11] Glötzel D and McMahan A K 1979 *Phys. Rev.* B **20** 3210
[12] McMahan A K 1984 *Phys. Rev.* B **29** 5982
[13] Skriver H L 1985 *Phys. Rev.* B **31** 1909
[14] Carlesi S, Frannchini A, Bortolani V and Martinelli S 1999 *Phys. Rev.* B **59** 11 716
[15] Andersen O K, Christensen N E, Pawlowska Z and Jepsen O 1987 unpublished
[16] Christensen N E, Boers D J, van Velsen J L and Novikov D L 2000 *Phys. Rev.* B **61** R3764
Christensen N E, Boers D J, van Velsen J L and Novikov D L 2000 *J. Phys.: Condens. Matter* **12** 3293
[17] Xie J, Chen S P, Tse J S, Klug D D, Li Z, Uehara K and Wang L G 2000 *Phys. Rev.* B **62** 3624
[18] Savrasov S Y 1992 *Phys. Rev. Lett.* **69** 2819
Savrasov S Y 1996 *Phys. Rev.* B **54** 16 470
[19] Savrasov S Y and Savrasov D Y 1996 *Phys. Rev.* B **54** 16 487
[20] Vosko S H, Wilk L and Nusair M 1980 *Can. J. Phys.* **58** 1200
[21] Perdew J P, Burke K and Ernzerhof M 1996 *Phys. Rev. Lett.* **77** 3865
[22] Blöchl P, Jepsen O and Andersen O K 1994 *Phys. Rev.* B **49** 16 223
[23] Born M and Huang K 1954 *Dynamical Theory of Crystal Lattices* (New York: Oxford University Press)
[24] Brockhause B N, Arase T, Caglioti G, Rao K R and Woods A D B 1962 *Phys. Rev.* **128** 1099